Reversible Bulk-Phase Change of Anthroyl Compounds for Photopatterning Based on Photodimerization in the Molten State and Thermal Back Reaction

Hideyuki Kihara* and Masaru Yoshida*

Nanosystem Research Institute (NRI), National Institute of Advanced Industrial Science and Technology (AIST), Tsukuba Central 5, 1-1-1 Higashi, Tsukuba, Ibaraki 305-8565, Japan

S *Supporting Information*

ABSTRACT: As new organic materials for rewritable photopatterning, 2-anthroyl and 9-anthroyl ester compounds were synthesized. Their bulk-phase changes (we use "bulk-phase change" as complete phase change in a mass of a material neither in a surface nor in a small quantity in this study) triggered by photodimerization under melting conditions (melt-photodimerization) and subsequent thermal back reactions were investigated. All the anthroyl compounds exhibited melting points lower than ca. 160 °C, and they were nearly quantitatively converted to the corresponding photodimers by UV irradiation at temperatures of ~5 °C higher than their respective melting points. We found that there were two kinds of bulk-phase change behaviors through the photoreaction. Two of the anthroyl compounds remained isotropic and lost fluidity during the melt-photodimerization. The obtained photodimers exhibited robust solid-state amorphous phases at room temperature. In contrast, the other three anthroyl compounds showed crystallization during the melt-photodimerization. The resulting photodimers changed from isotropic to crystalline phases, even at high temperature. Various experiments revealed that the bulk phase of the photodimers was affected not by the existence of regioisomers but by their fluidity at the photoirradiation temperature. The latter three photodimers retained enough fluidity, reflecting their high molecular mobilities at the photoirradiation temperature at which the isothermal crystallization occurred. The other two products were not able to crystallize due to low fluidity, resulting in amorphous phases. We also found that all the photodimers reverted to the corresponding monomers by thermal back reaction and recovered their initial photochemical and thermal properties. Using these reversible bulk-phase changes of the anthroyl compounds, we successfully demonstrated rewritable photopatterning in not only negative images but also positive ones, based on the optical contrast between the ordered and disordered phases.

KEYWORDS: anthracene, dimerization, photochemistry, phase transition, photopatterning
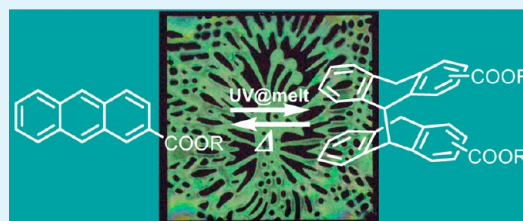
1. INTRODUCTION

Organic compounds that show unique electro-optic properties have attracted much attention because wet processes based on their solutions are applicable to the fabrication of various devices.[1−4] Anthracene and its derivatives are typical examples of the most well-known of such organic compounds, and their physical properties have been studied over a number of years.[5−8] Owing to their nature based on the delocalized π electrons of their fused-ring backbones, they have been proposed for applications in electronic devices such as organic light emitting diodes,[9−11] field effect transistors,[12−14] and solar cells.[15,16]

Another well-known facet of anthracenoid chemistry is their participation in photochemical dimerization reactions, which has been exploited for various functional materials, including photoinduced shape-change materials.[17−21] In addition, it was reported that anthracene-containing polymers were synthesized and used for photopatterning based on fluorescence contrast resulting from photodimerization of the anthracene moiety of the polymers.[22,23] However, little attention has been paid to the

reversible bulk-phase tuning of anthracene compounds based on photodimerization and subsequent thermal back reaction. The bulk-phase change of materials is expected to bring about significant alterations of their optical properties, such as light reflection and birefringence. Therefore, if the photoinduced phases are thermally stable, the material can be used as long-term optical data storage media. In addition, nondestructive reading of the storage data would be possible, because differences in the physical properties based on the phase change can be optically detected by light of a different wavelength from that used for photorecording by excitation.

In a previous study, we synthesized a liquid-crystalline (LC) compound having an anthroyl group at each terminus of the molecule and performed photopolymerization both in solution and the molten state through the intermolecular photo-dimerization of the anthroyl groups.[24] We found that the

resulting polymer with the photodimeric structure in the main chain was formed by sequential polymerization, and the product exhibited a thermally stable solid-state amorphous phase at room temperature. Furthermore, it was revealed that the polymer reverted to the initial α,ω-bisanthroyl monomer with LC and crystalline phases, when heated at around 230 °C. We also demonstrated photopatterning based on the contrast between the ordered and disordered phases of the anthracene monomers and polymers, respectively. However, taking advantage of the photopolymerization and thermal depolymerization for the phase change inevitably involved long response times. For example, it took as long as 12 h to obtain a polymer with sufficient molecular weight by photopolymerization in solution (solution-photopolymerization) in our previous study.[24] In addition, in the case of photopolymerization in the molten state (melt-photopolymerization), the α,ω-bisanthroyl molecule had to be heated to as high as 210 °C due to its high melting point (197 °C). Moreover, the photodimerization and the thermal back reaction of the resulting anthracene photodimer occurred very fast at such a high temperature, requiring that the heating temperature be gradually lowered from 210 to 130 °C at a cooling rate of 5 °C min to achieve enough conversion from the monomer to the polymer. As a result, at least 16 min was required for photochemical image recording with the α,ω-bisanthroyl compound. The very high temperature and image recording time (>10 min) were limitations from the viewpoint of practical processing.

In this study, we examined bulk-phase change for photopatterning based on photo*dimerization* instead of photo*polymerization* to improve upon the issues described above. For this purpose, we modified the monomer structure and synthesized five new *mono*anthroyl compounds, as shown in Figure 1. We then investigated the relationship between the
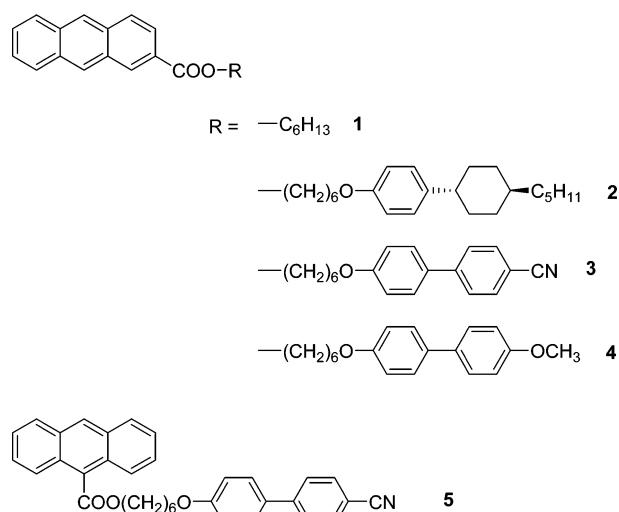

Figure 1. Chemical structures of 2- and 9-anthroyl compounds used in this study.

bulk-phase change of these compounds and the melt-photodimerization and thermal back reaction. If the phase change occurs, the response time for phase change based on photodimerization would be expected to be short compared to that based on the stepwise photopolymerization under relatively long photoirradiation times. Moreover, it would be easier to handle the monosubstituted compounds because the melting points of the monoanthroyl molecules are expected to

be lower than those of the bisanthroyl species due to their lower molecular weights.

As a result, two of the monoanthroyl compounds (**3**, **4**) in Figure 1 were converted into photodimers which showed solid-state amorphous phases upon melt-photoirradiation. Interestingly, the other three compounds (**1**, **2**, and **5**) exhibited isothermal crystallization via melt-photodimerization, which meant that the photodimer products had significantly high crystallinity and their crystalline phases could grow even at high temperature. Regardless of the difference of phase appearance behavior, all the obtained photodimers reverted to the initial monomers after heating at about 200 °C, as a result of the thermal back reaction. As a possible application of these photoresponsive materials, we successfully performed rewritable photopatterning using thin-layer samples of the monoanthroyl compounds.

2. EXPERIMENTAL SECTION

2.1. Materials. The syntheses of the anthroyl compounds in this study are described in the Supporting Information (Schemes S1−S3). 2-Anthracene carboxylic acid, 9-anthracene carboxylic acid, 4-cyano-4′-hydroxybiphenyl, 4-hydroxy-4′-methoxybiphenyl, 6-bromohexane, and 1,6-dibromohexane were purchased from Tokyo Chemical Industry Co., Ltd. (Japan). Dimethyl sulfoxide, acetone, and 1,8-diazabicyclo[5.4.0]undec-7-ene were purchased from Wako Pure Chemical Industries, Ltd. (Japan). 4-(Trans-4-*n*-pentylcyclohexyl)-phenol was purchased from Kanto Chemical Co., Inc. (Japan). All reagents were used without further purification.

2.2. General Methods. ^{1}H and ^{13}C NMR spectra were recorded on a JNM-ECX400 (JEOL, Japan) using $CDCl_3$ as the solvent and tetramethylsilane (TMS) as the internal standard. Matrix-assisted laser desorption ionization time-of-flight mass spectrometry (MALDI-TOF MS) was conducted using a Voyager-DE Pro instrument (Applied Bisosystems, USA) operated in reflector mode with 2,5-dihydroxybenzoic acid as a matrix. The thermal properties of the samples were evaluated by polarized optical microscopy (POM) using a BH2 (Olympus, Japan) equipped with an FP82HT hot stage (Mettler-Toledo, Japan) and by differential scanning calorimetry (DSC) using a DSC 6200 (Seiko Instruments Inc., Japan). Heating and cooling rates were 10 °C min^{-1}. For photoirradiation experiments, we prepared thin-layer samples from anthracene monomers. A predetermined weight (2 mg) of an anthracene monomer was placed between cover glasses and melted on an LK 600PH hot stage (Linkam Scientific Instruments, UK). To remove air bubbles, the molten sample was always pressed and spread over the whole area of the cover glass. Therefore, the thin-layer samples had almost the same thickness (ca. 10 μm), measured by a micrometer. Photoirradiation of the samples was carried out using monochromatic 365 nm UV light (5 mW cm^{-2}) from a 500 W high-pressure mercury lamp through optical filters. During photoirradiation, the temperature of the samples was controlled by an LK 600PH hot stage. The thermal back reaction was performed by the same hot stage. The thin layer samples, once photodimerized, were heated at a constant temperature for a prescribed period of time. After heating, the samples were analyzed by various measurements without purification. Gel permeation chromatography (GPC) was conducted using an LC-10ADvp pump unit, an SPD-10Avp UV detector (detection wavelength: 280 nm), a CTO-10Avp column oven, and an SCL-10Avp controller (Shimadzu, Japan) with Shodex KF800D and KF805L columns, using THF as the eluent. High-performance liquid chromatography (HPLC) was performed by a CCPM-II pump unit, a PD-8020 UV detector (detection wavelength: 290 nm), a CO-8020 column oven, and a PX-8020 controller (TOSOH, Japan) using a TSK silica-60 column. A mixed solution (toluene/dichloromethane/2-propanol = 90:10:0.2 v/v/v) was used as the eluent for the HPLC experiments. X-ray diffraction (XRD) analysis for photodimers was carried out by $2\theta/\theta$ method using a RIGAKU RINT2000 (RIGAKU, Japan).

3. RESULTS AND DISCUSSION

3.1. Thermal Properties of Monomers. Among the monoanthroyl compounds shown in Figure 1, only **1** was already known previously,[25,26] but its thermal and photochemical properties in the bulk state had not been reported. The commercially available starting materials for the syntheses of the anthracene derivatives, i.e., 2- and 9-anthracenecarboxylic acids, had melting points of 285.95 and 222.45 °C, respectively.[27] These melting points were too high to effectively perform the photodimerization because the reaction does not appear to proceed at such high temperatures due to the competitive thermal back reaction. Therefore, we prepared derivatives of the commercially available anthracene compounds. Rigid aromatic moieties, the so-called mesogens, were selected as appropriate substituents; in our previous study, a bisanthracene-functionalized mesogenic monomer was found to be important in the production of an amorphous-phase polymer.[24]

Table 1 shows the thermal properties of the monoanthroyl compounds. The esterification reaction effectively decreased

Table 1. Phase Transition Temperatures[a] (°C) of the Anthroyl Compounds

anthroyl compound	heating		cooling	
	g → Cr	Cr → I	I → Cr	I → g
1		92	82	
2		101	73	
3		143	110	
4		151	96	
5	65	144		4

[a]Determined by DSC; g: glassy; Cr: crystalline; I: isotropic.

the melting points of the products relative to the starting materials, probably owing to the lack of intermolecular hydrogen bonds. Note that only **5** showed, rather than crystallization, a glass transition at around 4 °C on cooling. Compound **5** also exhibited cold crystallization at 65 °C and subsequently melted at 144 °C on heating.

3.2. Bulk Phase of Photodimers Obtained by Melt-Photoirradiation. In a typical experimental procedure, a monoanthroyl compound (2 mg) from Figure 1 was placed between cover glasses (sample thickness: ca. 10 μm) and melted by heating at about 5 °C higher than the melting point. While maintaining that temperature, the sample was irradiated with UV light (365 nm, 5 mW cm^{-2}). The photodimerization products were analyzed by GPC, ^{1}H NMR, and MALDI-TOF MS. The experimental results showed that the anthroyl compounds were almost quantitatively converted to the corresponding photodimers within 30 min. Namely, minimum dose for the photodimerization of all amounts of monomers (2 mg) was estimated to be ca. 9 J cm^{-2}. As a representative example, a GPC chart of the photodimerization product of **3** is shown in Figure 2. As the irradiation time increased, the intensity of the peak at 12.8 min corresponding to **3** decreased, while the new peak for the photodimer appeared at 12.1 min with gradually increasing intensity.

The phases of the resulting photodimers determined by not only POM observations but also XRD measurements at room temperature are listed in Table 2 (XRD profiles of photodimers are given in Figure S1 in the Supporting Information). We found that the photodimerization of the monoanthroyl
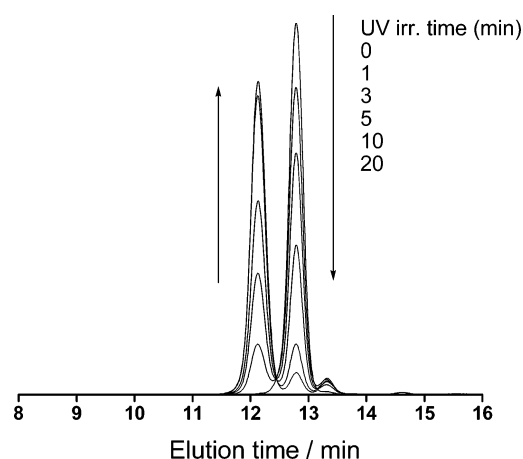
Figure 2. GPC charts of **3** obtained by UV irradiation in the molten state at 150 °C for various periods of time.

Table 2. Phase State of the Photodimers[a] at Room Temperature

starting anthroyl compound	phase state of the photodimer at room temperature
1	inhomogeneous crystal
2	inhomogeneous crystal
3	solid-state amorphous
4	solid-state amorphous
5	homogeneous crystal

[a]Obtained by UV irradiation of the corresponding monomer in the molten state for 30 min.

compounds actually worked well for bulk-phase change. For example, the isotropic phases of **3** and **4** induced by the photodimerization were formally maintained during photoirradiation, and the amorphous phases were preserved at room temperature. The amorphous phases were formed regardless of the rate of the cooling processes after UV irradiation, i.e., rapid (irradiated sample was placed on a metal plate at room temperature) or slow (2 °C min^{-1}) cooling using a temperature controller. The appearances of the irradiated samples of **3**, both rapidly and slowly cooled, were colorless and transparent (Figure 3). The cooling-rate independent results for the bulk phases suggested that the solid-state amorphous phases of the photodimers were not kinetically formed metastable states but were thermodynamically stable ones.
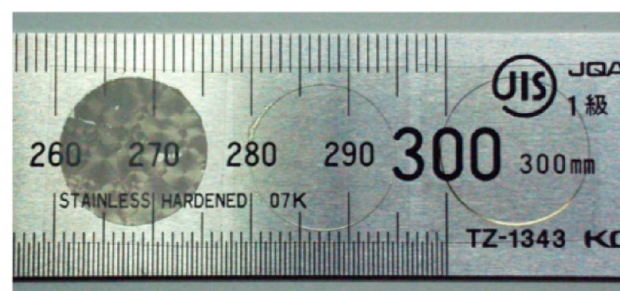
Figure 3. Photographs of **3** before UV irradiation (left). Photodimer obtained by UV irradiation of **3** in the molten state with subsequent rapid cooling (middle) or slow cooling (right), respectively. The circular samples were placed on a ruler.

2652

dx.doi.org/10.1021/am400111q | ACS Appl. Mater. Interfaces 2013, 5, 2650−2657

On the other hand, crystalline phases were generated during the photoirradiation of **1**, **2**, and **5** under high temperature conditions, and the crystals of the corresponding photodimers were maintained throughout the cooling process to room temperature. For instance, many small crystal grains were clearly seen in irradiated **1** by POM, as shown in Figure 4. A
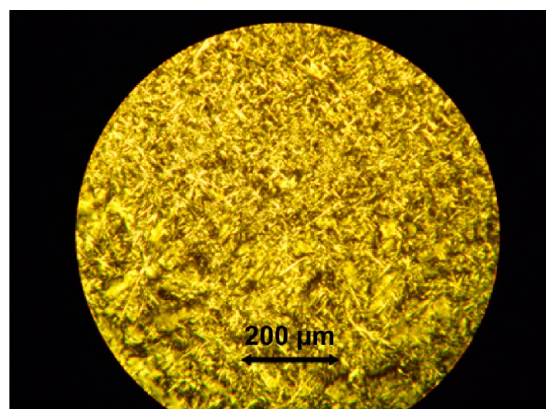

Figure 4. POM image of photodimer obtained by UV irradiation of **1** in the molten state.

similar POM image showing crystals was observed for the irradiated sample of **2**. While 9-substituted anthracene **5** has a cyanobiphenyl mesogen akin to **3** showing an amorphous phase in the photodimer, crystalline areas were generated and spread in the molten amorphous sample during the photoirradiation at 150 °C. Eventually, the whole irradiated sample was covered by crystals of the photodimer of **5** after 15 min, even at high temperature. The growth of the crystalline phase during the photoirradiation is shown in Figure 5. The crystallization
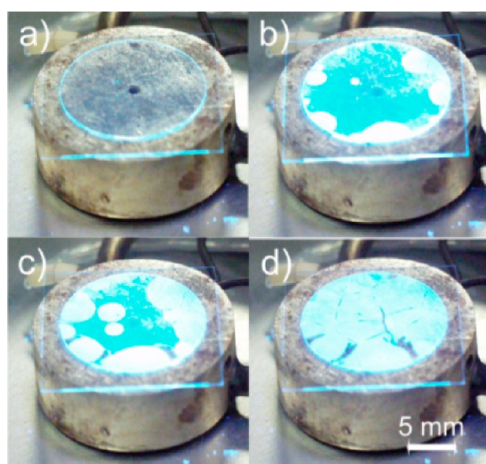

Figure 5. Photographs of crystal growth in the molten sample of **5** taken (a) 0, (b) 8, (c) 10, and (d) 15 min after the beginning of UV irradiation.

behaviors arising from the photodimerizations of **1**, **2**, and **5** indicated that the resulting photodimers had very high crystallinity and their crystals, once formed, did not melt at the melting point of the corresponding monomer. Note that, whereas the crystalline phases of the photodimers derived from **1** and **2** consisted of small crystalline domains, as already mentioned, a homogeneous and large crystal domain was formed in the photodimer of **5**, as observed by POM (Figure

6). We assume the difference in the crystal structures would be derived from the regioselectivity of the reaction, because 9-
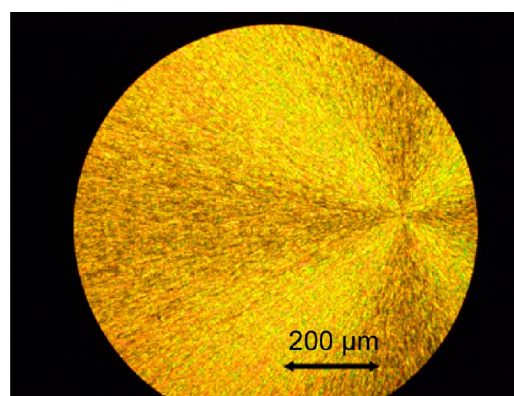

Figure 6. POM image of photodimer obtained by UV irradiation of **5** in the molten state.

anthroyl compounds are likely to form head-to-tail dimers.[28] Later, we will discuss the relationship between the bulk phase and the regioselectivity issue.

3.3. Thermal Back Reactions of Photodimers. As mentioned, there were two groups of photodimers: one showed an amorphous phase and the other was crystalline. First, the thermal back reaction of the amorphous phase-type anthracene photodimer of **3** was examined using a hot stage, and the reaction process was investigated by GPC and ^{1}H NMR measurements. As shown in the GPC charts (Figure 7),
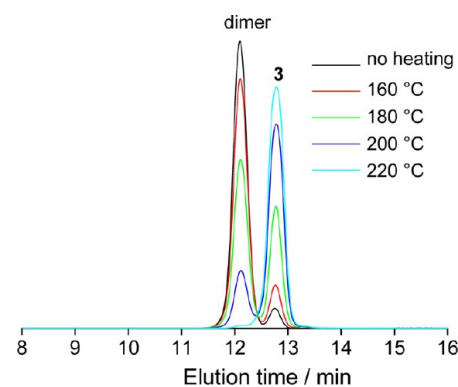

Figure 7. GPC charts of photodimer obtained by UV irradiation of **3** in the molten state for 30 min, measured after heating at various temperatures for 5 min.

the higher the heating temperature of the photodimer, the faster was the thermal back reaction. The photodimer almost quantitatively reverted to the initial anthroyl monomer within 5 min upon heating at 220 °C. In the ^{1}H NMR spectra corresponding to the dimerization and back reactions (Figure 8), the peaks associated with the anthracene moiety in monomer **3** (a, b, c in Figure 8a) disappeared in the spectrum of the photodimer (Figure 8b) and reappeared in the spectrum of the regenerated monomer **3** (Figure 8c). Similarly, a new peak appeared at 4.63 ppm, which corresponded to the bridge-head proton in the spectrum of the photodimer (indicated by a dot in Figure 8b), and then vanished after the thermal back reaction (Figure 8c). The regenerated monomer **3** was found to crystallize at room temperature. Moreover, the regenerated monomer was again converted to the photodimer by
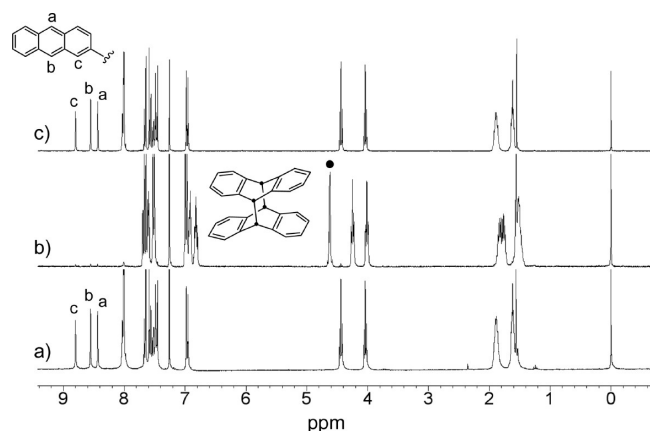
2653

dx.doi.org/10.1021/am400111q | ACS Appl. Mater. Interfaces 2013, 5, 2650−2657

Figure 8. ^{1}H NMR spectra of (a) **3**, (b) photodimer obtained by UV irradiation of **3** in the molten state for 30 min, and (c) the regenerated monomer **3** obtained by heating the photodimer at 220 °C for 5 min.

photoirradiation in the molten state. Compound **4** displayed similar reproducibility.

Second, when the crystalline photodimers obtained by the melt-photoirradiation of **1**, **2**, and **5** were heated at around 200 °C in a manner similar to **3**, they eventually changed to the isotropic phase. ^{1}H NMR and GPC measurements of the heated samples revealed that the formation of the isotropic phase could not be ascribed to melting. Instead, the corresponding monomers were regenerated by the thermal back reactions (GPC charts of **1** and **5** are given in Figure S2 in the Supporting Information). These results indicated that the photodimers of **1**, **2**, and **5** did not have actual melting points because, on heating, the thermal back reaction occurred prior to melting. The crystals of the photodimers were directly converted to the corresponding molten monomers when heated at around 200 °C. The regenerated monomers had photochemical and thermal properties identical to the original ones. Therefore, in the thermal back reaction, there was no difference in the reactivity of the amorphous and crystalline photodimers; each returned its initial monomer.

3.4. HPLC Analysis of Photodimers. To investigate the effect of the photodimerization regioselectivity on the bulk phase of the photodimers, high-performance liquid chromatography (HPLC) analysis of the corresponding products was performed. The photodimers of **1**, **2**, and **5**, which showed crystalline phases, were collected before completion of the photodimerization (irradiation time: 10 min) for HPLC analysis. The results are shown in Figure 9. In the case of 9-anthroyl monomer **5**, not only the peak of monomer **5** at around 5.75 min but also the peak of the photodimer at about 7.26 min was detected in the HPLC chart. The formation of two regioisomers, i.e., the head-to-head (HH) and head-to-tail (HT) isomers, as shown in Figure 10a, was theoretically expected in the photodimerization of **5**. However, only one peak was actually observed by HPLC. In the ^{1}H NMR spectrum, we observed a simple pattern of peaks, which suggested regioselective product formation. In addition, a HH dimer derived from a 9-substituted anthracene was previously reported to be thermally unstable compared to the HT dimer.[28] The present result thus should indicate that, even if the HH isomer was photochemically formed, it would likely decompose to the monomer by the thermal back reaction under the molten conditions. Consequently, the HT isomer would become the sole product from the photoirradiation of **5**. The formation of a
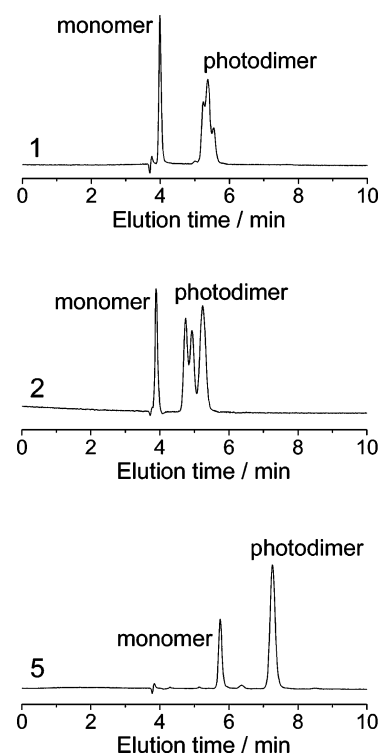

Figure 9. HPLC charts of **1**, **2**, and **5** measured after UV irradiation in their molten states for 10 min.
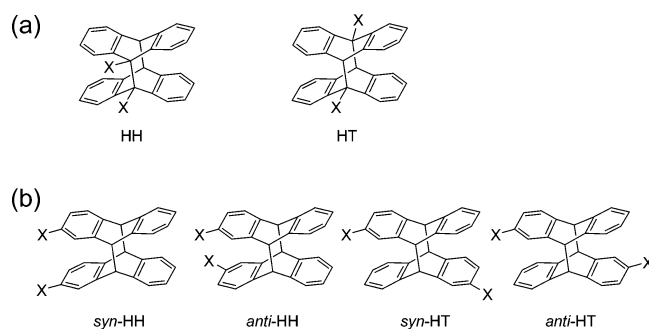

Figure 10. Chemical structures of possible photodimer regioisomers obtained from (a) 9-anthroyl and (b) 2-anthroyl compounds.

single product upon the photoirradiation of **5** was probably the main reason why the homogeneous crystalline domain, as already shown in Figure 6, grew during the treatment.

In the cases of the 2-anthroyl monomers **1** and **2**, four regioisomers, i.e., *syn*-HH, *anti*-HH, *syn*-HT, and *anti*-HT isomers, can be formed during photoirradiation (Figure 10b). In the event, three photodimer peaks were detected in both HPLC charts of **1** and **2**, as shown in Figure 9. The three peaks observed among the four possible suggested that the photodimerization of **1** and **2** was not completely random but was essentially nonregioselective. It was rather interesting that the photodimers of the two compounds showed thermally stable crystalline phases at the relatively high temperature in spite of the lack of regioselectivity as confirmed by HPLC. We believe that the formation of photodimer mixtures with at least three isomers is a possible reason for the relatively inhomogeneous domains of the crystalline phases in the photodimers derived from **1** and **2**, as compared to **5**, and already depicted in Figure 4.

We also found that the amorphous-phased photodimers of **3** and **4** comprised a mixture of regioisomers, similarly to **1** and **2** (Figure S3 in the Supporting Information). In these cases, the lack of regioselectivity may affect the induction of the thermally stable amorphous phase. In the next section, we will discuss the possible mechanism for the bulk-phase preference of the photodimers between amorphous and crystalline states.

3.5. Possible Mechanism for Structure-Dependent Solid-State Phase Formation of Photodimers. Even though the photodimers derived from **1** and **2** were mixtures of regioisomers, they exhibited isothermal crystallization behaviors during photodimerization. In contrast, the melt-photoirradiation of **3** and **4** resulted in the formation of a solid-state amorphous phase as well as a mixture of regioisomers, similarly to **1** and **2**. We consider that the vitrification behavior of the photodimers of **3** and **4** can be attributed to their poor molecular mobility at the photoirradiation temperature, which is supported by the following observations. A DSC experiment performed for the photodimer derived from **3** revealed that no exothermic peak corresponding to a cold crystallization, which needs some degree of molecular mobility for intermolecular rearrangement, was observed on heating to 200 °C (Figure S4 in the Supporting Information). Also, the photodimer did not soften, even beyond 150 °C. These observations should indicate that the photodimer of **3** had low fluidity based on poor molecular mobility at the relatively high photoirradiation temperature. It has been reported that decreased molecular mobility frequently suppresses the crystallinity of organic compounds in the cases of polymer materials.[29,30] We consider that a similar suppression of crystallinity related to low molecular mobility may occur with the photodimers of **3** and **4**, resulting in amorphous phases.

On the other hand, to examine the importance of molecular mobility on the isothermal crystallization of the anthracene photodimer, we prepared glassy and amorphous samples of **5** by supercooling from the molten state followed by photo-irradiation at room temperature. First, we investigated the relationship between the photoirradiation time and the conversion from **5** to the photodimer. The conversion reached equilibrium at ca. 80% in 1 h, maintaining the glassy phase at room temperature. However, when the irradiated sample was heated at 150 °C for several minutes, the amorphous phase was smoothly changed into the crystalline phase (Figure S5 in the Supporting Information). This result suggested that sufficient molecular mobility at the higher temperature (150 °C) could trigger organization into the more thermally stable crystalline phase than the amorphous one.

From the results so far obtained, we propose that the reason why the melt-photodimerization of **3** and **4** resulted in the formation of solid-state amorphous phases is as follows. By analogy with the photodimers of **1**, **2**, and **5**, it was assumed that the photodimers of **3** and **4** would have the potential to form crystalline phases during photodimerization at higher temperatures. However, the molecular mobilities of the photodimers of **3** and **4** at the photoirradiation temperature were too low to change into a crystalline phase. Therefore, the amorphous phases of the photodimers did not alter and were preserved at room temperature. Because the origin of the low molecular mobilities of **3** and **4** despite their structural similarities with the other anthroyl monomers is not yet clear, additional and rational studies are ongoing.

Actually, we first synthesized **3** having a cyanobiphenyl mesogen among the five anthroyl monomers, because we had

searched LC compounds which could be photodimerized without a sensitizer. We had studied LC cinnamoyl compounds and found that a sensitizer was important for efficient photodimerization of them.[31,32] While **3** did not show LC phases, it exhibited the reversible crystalline−amorphous phase change based on photodimerization and thermal back reaction. We were significantly interested in this phenomenon and synthesized the analogous anthroyl compounds to clarify necessary conditions for the reversible-phase change. Whereas the kind of mesogens and the substitution position in the anthracene backbone were varied, the structural variations are still limited to elucidate a relationship between the chemical structure and the phase state of the photodimers in Table 2. It is known that other acene molecules, such as tetracene and pentacene, also undergo photodimerization and thermal back reaction.[33,34] Therefore, it may be possible to use such acene moieties for preparation of phase-changeable materials; however, anthracene structure is considered to be superior from the viewpoint of synthetic approach.

3.6. Rewritable and Negative−Positive Photopatterning Using Monoanthroyl Compounds. Among the five anthroyl compounds, we verified that reversible-phase change between the crystalline and solid-state amorphous phases took place in **3** by the combination of light and heat. Therefore, we performed a photopatterning demonstration using **3** as follows. Before carrying out the photopatterning, we examined the relationship between the conversion from the monomer **3** to the photodimer and the bulk phase of the irradiated sample at room temperature. A small amount of **3** (2 mg) was placed between cover glasses and melted at 150 °C. The sample was then irradiated by UV light (365 nm, 5 mW cm^{-2}) at 150 °C and cooled to room temperature to analyze the solid-state phase. It was found that at least 20% conversion was necessary to obtain a completely amorphous-phased sample. This suitable conversion number was achieved by photoirradiation for at least 5 min. Therefore, the photopatterning of **3** was conducted using 5 min photoirradiation with a metallic bookmark as a photomask (Figure 11a). The image of the obtained sample under polarized light is shown in Figure 11b. The contrast in the photopattern was based on the difference between the amorphous phase of the irradiated area and the ordered phase of the unirradiated area. Both the recording temperature and time for **3** (150 °C, 5 min) were reduced compared to those used for the melt-photopolymerization of the previously studied bisanthracene molecule, for which 210 °C as the maximum temperature and 16 min as a recording time were necessary.[24]

The photopattern was easily erased by the thermal back reaction and crystallization of the whole sample on heating at 220 °C for 2 min. In contrast to the image writing temperature as described above, that required for erasing could not be reduced compared to the α,ω-bisanthroyl compound. This is because the backbone structure of the anthracene photodimer of **3** was basically the same as that of the previously described anthracene photopolymer, which determines the reactivity of the thermal back reaction.[7] After erasing the first photopattern, another photopattern was recorded in the regenerated crystalline sample by the same procedure but using a different photomask (Figure 11c,d). The erasing and rewriting processes were repeatable several times (note that thermal decomposition of **3** gradually occurs). In addition, the photopattern was clearly maintained under ambient conditions for over two years. This remarkable preservation was ascribed to both the photo-
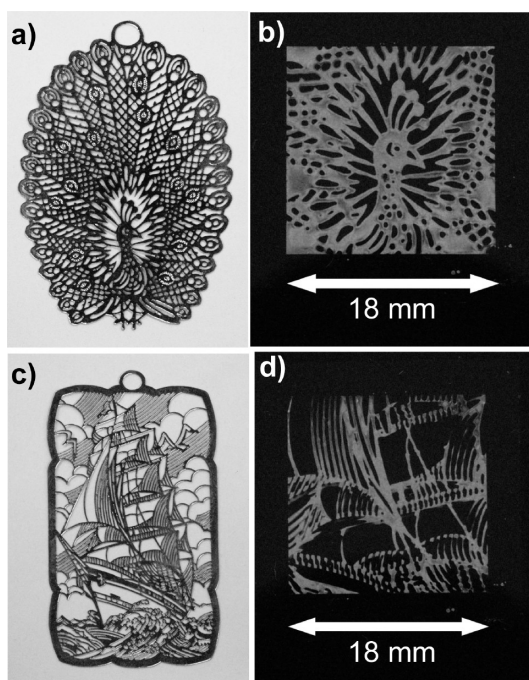
2655

dx.doi.org/10.1021/am400111q | ACS Appl. Mater. Interfaces 2013, 5, 2650−2657

Figure 11. (a) Metallic bookmark used as the first photomask. (b) Photopatterning image written in the thin layer sample of **3**. (c) Bookmark used as the second photomask. (d) Photopatterning image rewritten in sample (a) after erasure by thermal back reaction.

chemical and thermal stability of the solid-state amorphous phase formed in the photoirradiated sample.

To investigate the spatial resolution limit in the photo-patterning, a thin layer sample of **3** was irradiated with UV light (365 nm, 5 mW cm^{-2}, 5 min) through a photomask with a test pattern (Figure 12a). POM image of the obtained sample
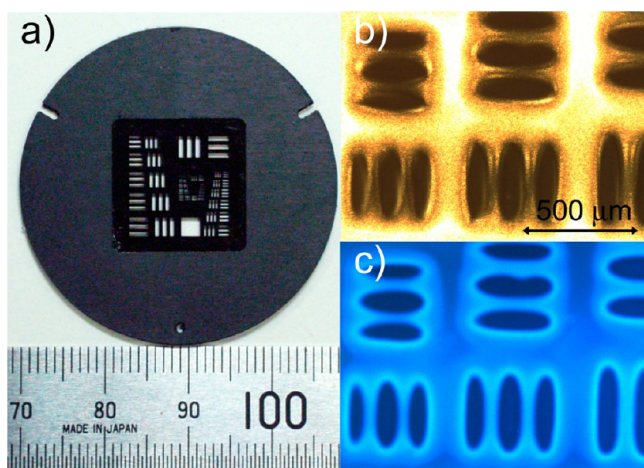

Figure 12. (a) Photomask with a test pattern used for photo-patterning. (b) POM image of the thin layer sample of **3** patterned using the photomask. (c) Fluorescence microscopic image observed in the same area as the POM image.

revealed that the resolution limit was ca. 50 μm in the condition used in this study (Figure 12b). If the photopatterning condition, such as intensity of irradiation light, will be optimized, it would be possible to improve the resolution by the reduction of the recording time. We also obtained a patterned image of the same sample by fluorescence

microscopy (Figure 12c). The dark areas of the POM image, i.e., amorphous areas, corresponded with those of the fluorescence image. This observation was reasonable because the photodimer lost the π-conjugated structure and no longer emitted fluorescence.[22]

Interestingly, negative images corresponding to the photo-patterns of **3** were obtained using **5** instead of **3**. When a thin layer sample of **5** between cover glasses was irradiated with UV light (365 nm, 5 mW cm^{-2}) through the photomask in the molten state, the irradiated parts of the sample gradually crystallized within about 15 min. After cooling to room temperature, the crystal phase remained but the unirradiated parts of the sample exhibited the amorphous phase due to supercooling, as described in a previous section. The crystalline and amorphous areas corresponded to the UV-irradiated and unirradiated parts, respectively (Figure 13). The photopattern
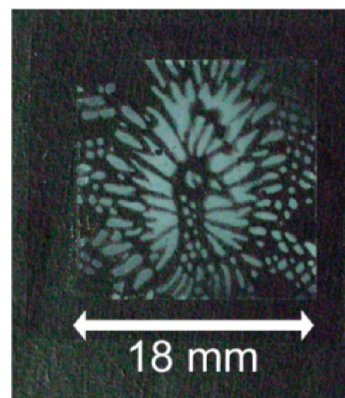

Figure 13. Photopatterning image written in the thin layer sample of **5** obtained by UV irradiation for 15 min through the photomask.

was simply the negative of that obtained from **3**. Compared with the photopatterns made by **3**, those obtained from **5** had less clear edges owing to a recording time that was longer by 10 min than that of **3**. The images by **5** also became blurred in a few days due to the thermal crystallization of the amorphous region kinetically induced by supercooling. However, rewriting was still available on the same sample of **5**, indicating a possible temporal use as an image visualized medium.

4. CONCLUSIONS

We synthesized five derivatives of 2- and 9-anthroyl compounds with various substituents and investigated their bulk-phase changes induced by melt-photodimerizations and thermal back reactions. Although all the anthroyl compounds were quantitatively converted to the corresponding photodimers by melt-photoirradiation, their bulk phases strongly depended on their molecular structures. For instance, 2-anthroyl compounds with 4-cyanobiphenyl substituents afforded photodimers that exhibited solid-state amorphous phases at room temperature. In contrast, melt-photoirradiation of a 2-anthroyl compound with a hexyl substituent resulted in isothermal crystalline-phase formation. From the various experimental results, we considered that the bulk phase of the photodimers obtained by melt-photodimerization was affected by their fluidity, based on the molecular mobility of the photodimers. If the photodimer had enough fluidity at the photoirradiation temperature, it isothermally reorganized into the crystalline phase. In contrast, when the fluidity of the photodimer was not

sufficient at the photoirradiation temperature, the isotropic phase did not change and was preserved at room temperature. All the photodimers reverted to the initial anthroyl monomers by heating due to the thermal back reaction, and the resulting monomers had thermal properties identical to the pristine monomers. We thus demonstrated rewritable photopatterning by choosing suitable anthracene compounds. Photoirradiation through a photomask resulted in area-selective phase changes in thin-layer samples of the anthroyl compounds. Both the photoimage writing temperature and time were reduced to some extent for these anthroyl compounds as compared to the previously reported bisanthroyl molecule. Moreover, we obtained both positive and negative photopatterns by the appropriate choice of anthroyl compounds.

The reversible-phase change of organic compounds, as investigated in the present study, will be applied to functional materials such as imaging and photostorage media. This study revealed the basic concept and unique potential of anthracene compounds as new materials for rewritable photopatterning. Studies on further improvements in the nature of the anthroyl compounds for practical uses are now in progress.

■ ASSOCIATED CONTENT

Ⓢ Supporting Information

Syntheses of the anthroyl compounds; XRD profiles of photodimers of **1**, **3**, and **5**; GPC charts of the thermal back reactions of the photodimers of **1** and **5**; HPLC charts of photodimers of **3** and **4** prepared by melt-photoirradiation; DSC thermogram of photodimer of **3**; photographs of phase behavior of **5** when photoirradiated in the glassy phase. This material is available free of charge via the Internet at http://pubs.acs.org.

■ AUTHOR INFORMATION

Corresponding Author
*E-mail: h-kihara@aist.go.jp (H.K.); masaru.yoshida@aist.go.jp (M.Y.).
Notes
The authors declare no competing financial interest.

■ ACKNOWLEDGMENTS

■ REFERENCES

(1) Horii, Y.; Ikawa, M.; Chikamatsu, M.; Azumi, R.; Kitagawa, M.; Konishi, H.; Yase, K. *ACS Appl. Mater. Interfaces* **2011**, *3*, 836−841.

(2) Kambayashi, T.; Wada, H.; Goto, M.; Mori, T.; Park, B.; Takezoe, H.; Ishikawa, K. *Org. Electron.* **2006**, *7*, 440−444.

(3) Wang, Z.; Lou, Y.; Naka, S.; Okada, H. *ACS Appl. Mater. Interfaces* **2011**, *3*, 2496−2503.

(4) Xu, Q.; Chen, H. Z.; Wang, M. *Mater. Chem. Phys.* **2004**, *87*, 446−451.

(5) Becker, H. D. *Chem. Rev.* **1993**, *93*, 145−172.

(6) Bouas-Laurent, H.; Castellan, A.; Desvergne, J.-P.; Lapouyade, R. *Chem. Soc. Rev.* **2000**, *29*, 43−55.

(7) Bouas-Laurent, H.; Castellan, A.; Desvergne, J.-P.; Lapouyade, R. *Chem. Soc. Rev.* **2001**, *30*, 248−263.

(8) Wright, W. H. *Chem. Rev.* **1967**, *67*, 581−597.

(9) Huang, J. H.; Su, J. H.; Tian, H. *J. Mater. Chem.* **2012**, *22*, 10977−10989.

(10) Danel, K.; Huang, T. H.; Lin, J. T.; Tao, Y. T.; Chuen, C. H. *Chem. Mater.* **2002**, *14*, 3860−3865.

(11) Kim, Y. H.; Jeong, H. C.; Kim, S. H.; Yang, K. Y.; Kwon, S. K. *Adv. Funct. Mater.* **2005**, *15*, 1799−1805.

(12) Klauk, H.; Zschieschang, U.; Weitz, R. T.; Meng, H.; Sun, T.; Nunes, G.; Keys, D. E.; Fincher, C. R.; Xiang, Z. *Adv. Mater.* **2007**, *19*, 3882−3887.

(13) Ando, S.; Nishida, J.; Fujiwara, E.; Tada, H.; Inoue, Y.; Tokito, S.; Yamashita, Y. *Chem. Mater.* **2005**, *17*, 1261−1264.

(14) Meng, H.; Sun, F. P.; Goldfinger, M. B.; Jaycox, G. D.; Li, Z. G.; Marshall, W. J.; Blackman, G. S. *J. Am. Chem. Soc.* **2005**, *127*, 2406−2407.

(15) Valentini, L.; Bagnis, D.; Marrocchi, A.; Seri, M.; Taticchi, A.; Kenny, J. M. *Chem. Mater.* **2008**, *20*, 32−34.

(16) Mikroyannidis, J. A.; Stylianakis, M. M.; Balraju, P.; Suresh, P.; Sharma, G. D. *ACS Appl. Mater. Interfaces* **2009**, *1*, 1711−1718.

(17) Li, T. S.; Chen, J. F.; Mitsuishi, M.; Miyashita, T. *J. Mater. Chem.* **2003**, *13*, 1565−1569.

(18) Wang, C.; Zhang, D. Q.; Xiang, J. F.; Zhu, D. B. *Langmuir* **2007**, *23*, 9195−9200.

(19) Zheng, Y. J.; Mieie, M.; Mello, S. V.; Mabrouki, M.; Andreopoulos, F. M.; Konka, V.; Pham, S. M.; Leblanc, R. M. *Macromolecules* **2002**, *35*, 5228−5234.

(20) Goldbach, J. T.; Russell, T. P.; Penelle, J. *Macromolecules* **2002**, *35*, 4271−4276.

(21) Al-Kaysi, R. O.; Bardeen, C. J. *Adv. Mater.* **2007**, *19*, 1276−1280.

(22) Rameshbabu, K.; Kim, Y.; Kwon, T.; Yoo, J.; Kim, E. *Tetrahedron Lett.* **2007**, *48*, 4755−4760.

(23) Kim, J.; Anand, C.; Talapaneni, S. N.; You, J.; Aldeyab, S. S.; Kim, E.; Vinu, A. *Angew. Chem., Int. Ed.* **2012**, *51*, 2859−2863.

(24) Kihara, H.; Motohashi, M.; Matsumura, K.; Yoshida, M. *Adv. Funct. Mater.* **2010**, *20*, 1561−1567.

(25) Boens, N.; Debrackeleire, M.; Huybrechts, J.; Deschryver, F. C. *Z. Phys. Chem.-Frankfurt* **1976**, *101*, 417−428.

(26) Vanderauwera, P.; Deschryver, F. C.; Weller, A.; Winnik, M. A.; Zachariasse, K. A. *J. Phys. Chem.* **1984**, *88*, 2964−2970.

(27) Goldfarb, J. L.; Külaots, I. *J. Therm. Anal. Calorim.* **2010**, *102*, 1063−1070.

(28) Ito, Y.; Fujita, H. *J. Org. Chem.* **1996**, *61*, 5677−5680.

(29) Huo, P.; Cebe, P. *Macromolecules* **1992**, *25*, 902−909.

(30) Wang, L.; Fang, P.; Ye, C.; Feng, J. *J. Polym. Sci., Part B: Polym. Phys.* **2006**, *44*, 2864−2879.

(31) Kihara, H.; Tamaoki, N. *Macromol. Rapid Commun.* **2006**, *27*, 829−834.

(32) Kihara, H.; Tamaoki, N. *Liq. Cryst.* **2007**, *34*, 1337−1347.

(33) Berg, O.; Chronister, E. L.; Yamashita, T.; Scott, G. W.; Sweet, R. M.; Calabrese, J. *J. Phys. Chem. A* **1999**, *103*, 2451−2459.

(34) Bénard, C. P.; Geng, Z.; Heuft, M. A.; VanCrey, K.; Fallis, A. G. *J. Org. Chem.* **2007**, *72*, 7229−7236.